RSC Advances

PAPER

View Article Online
View Journal | View Issue

Cite this: *RSC Adv.*, 2022, **12**, 8833

Dendritic structured palladium complexes: magnetically retrievable, highly efficient heterogeneous nanocatalyst for Suzuki and Heck cross-coupling reactions†

Safoora Sheikh, [ab] Mohammad Ali Nasseri, *[a] Mohammad Chahkandi, *[c] Oliver Reiser [b] and Ali Allahresani [a]

The recyclable nanomagnetic Pd-complex PAMAM G_0-Pd@γ-Fe_2O_3 is reported for catalytic C–C cross-coupling reactions of challenging substrates. Mainly, a great variety of aryl chlorides can be used as substrates for Suzuki–Miyaura and Mizoroki–Heck reactions under mild reaction conditions (60–90 °C) and low catalyst loading (<1 mol% Pd) in aqueous media. The presence of numerous polar groups in the polymer matrix increases the solubility of the catalyst in water, thus facilitating its operation in aqueous environments. The immobilization of the catalyst on the surface of a magnetic platform allows its effective recovery and reuse without significant loss of catalytic activity for at least six cycles with total leaching of <1% palladium metal, meeting the requirements for acceptable metal residues in the pharmaceutical industry.

Received 23rd January 2022
Accepted 8th March 2022

DOI: 10.1039/d2ra00487a

rsc.li/rsc-advances

1. Introduction

The development of new protocols and methods according to green chemistry standards to meet the growing demands of human society for energy, health, and agricultural purposes remains a pressing challenge for chemistry and the related sciences.[1,2] Arguably, catalysis stands at the forefront of such efforts, providing innovation by the development of new chemical transformations. Nevertheless, making catalysis feasible for large-scale applications by improving catalytic activity and selectivity, and especially in the case of transition metal catalysis, obviating metal leaching is equally essential even for well-established transformations.[3]

In this context, palladium-catalyzed cross-couplings have been manifold proven to be of particular significance for synthesizing medicinally relevant compounds even though palladium is one of the scarcest metals in the world.[4–6] Efficient recycling of such species is economically desirable; moreover, the considerable toxicity of palladium mandates its removal below 10 ppm in pharmaceuticals.[7] Separating homogeneous palladium catalysts from products is challenging; consequently, heterogenization of palladium catalysts is a viable approach to overcome these difficulties. However, typical heterogeneous palladium catalysts such as Pd/C, being most successful for hydrogenations,[8] are less efficient in cross-coupling reactions, especially with industrially relevant aryl chlorides.[9] Such substrates remain challenging with any catalyst despite some impressive advances in designing molecular palladium complexes with specialized ligands.[10–17]

Considering large-scale and recycling, many efforts have been made to develop heterogeneous Pd-catalysts,[10–14] including molecular palladium–ligand complexes deposited onto various solid supports.[15–19] Among them, iron oxide nanoparticles have emerged as an attractive platform for metal catalysts[20] and especially for palladium complexes to arrive at eco-friendly and robust heterogeneous catalysts for Suzuki–Miyaura and Heck–Mizoroki C–C cross-coupling reactions.[21–24] Such catalysts can be easily manipulated and retrieved by external magnets avoiding cumbersome centrifugation or filtration processes.[25–27] Moreover, iron oxide nanoparticles have a high surface-to-volume ratio, which allows generating a large number of active sites that are available to promote catalytic reactions.[28,29]

Polyamidoamine (PAMAM) dendrimers have a particularly well-defined structure favorable for the encapsulation of metal nanoparticles.[30] The nanoparticle size and the metal loading can be controlled by the dendrimer generation, whereas the solubility in common solvents can be adjusted by the nature of the dendritic end group.[31] Despite these attractive properties, dendrimers are often difficult to recycle and to reuse; thus, attaching them to magnetic supports holds the promise to

[a]*Department of Chemistry, Faculty of Basic Sciences, University of Birjand, P. O. Box 97175-615, Birjand, Iran. E-mail: manaseri@birjand.ac.ir*

[b]*Institut für Organische Chemie, Universität Regensburg, Universitätsstr. 31, 93053 Regensburg, German*

[c]*Department of Chemistry, Faculty of Basic Sciences, Hakim Sabzevari University, P. O. Box 96179-76487, Sabzevar, Iran. E-mail: m.chahkandi@hsu.ac.ir*

† Electronic supplementary information (ESI) available. See DOI: 10.1039/d2ra00487a

combine tunability of the dendritic core to generate a suitable environment of catalytically active moieties with magnetic properties beneficial for recovery and reuse.[32]

Previously, various homogeneous and heterogeneous systems of palladium nanoparticles encapsulated in modified PAMAM dendrimers of generation G_2–G_6 have been reported for Suzuki–Miyaura and Mizoroki–Heck cross-coupling reaction.[33–36] For example, PAMAM-G_3 grafted on functionalized multiwall carbon nanotubes (MWCNTs-NH_2) showed good activity for aryl chlorides in Heck reactions employing *N*-methyl-2-pyrrolidone (NMP) as a solvent,[33] and the Fe_3O_4-G_4-PAMAM-Pd(0) could convert aryl chlorides in DMF as a solvent in Suzuki–Miyaura couplings.[34] Moving towards environmentally more benign solvent systems, the G_6-OH($Pd_{74}Cu_{73}$) PAMAM[34] dendrimer or Fe_3O_4@SiO_2-PAMAM-Pd[36] were competent catalysts for aryl chlorides in Suzuki–Miyaura reactions in a mixture of EtOH/H_2O. Similar to the PAMAM structure, polypropylene polybenzyl isocyanate (PPI) dendrimers modified by diphosphines as coordination site for Pd(II) complex have been employed successfully in Suzuki–Miyaura reactions with aryl chlorides in a THF/H_2O solvent mixture.[37] More Pd-PAMAM-based systems were reported, but these only catalyze the coupling of aryl iodides and bromides effectively and show little activity at best for aryl chlorides.[38–42]

We report here the synthesis of a hybrid material, consisting of a superparamagnetic γ-Fe_2O_3 core decorated with zero-generation PAMAM dendrimer G_0 in which palladium nanoparticles were encapsulated (Fig. 1). This catalytic system shows unusual high activity for Suzuki–Miyaura and Heck coupling reactions, most notably with a wide variety of aryl chlorides as substrates.

2. Experimental section

The preparation of PAMAM G_0-Pd@γ-Fe_2O_3 nanocatalyst is described in detail in the experimental section (ESI, Section 1. Schemes 1–3†). Briefly, at first γ-Fe_2O_3 nanocore was prepared as the platform for the immobilization, using Fe(II) and Fe(III) chloride salts. Then the iron oxide nanoparticles were functionalized with (3-chloropropyl)triethoxysilane followed by the attachment of the zero-generation of polyamidoamine dendrimer (PAMAM) to the γ-Fe_2O_3 MNPs through the siloxy linker. Subsequently, PAMAM G_0@γ-Fe_2O_3 was treated with palladium dichloride, which produced the PAMAM G_0-Pd@γ-Fe_2O_3 (ESI, Schemes 1–3†). The physicochemical properties of PAMAM G_0-Pd@γ-Fe_2O_3 were characterized by FT-IR, TEM, XRD, FE-SEM, ICP, TGA/DTG, VSM, MAP, XPS, EDS, and LC-MS analyzes (see the ESI, Fig. S1–S16†).

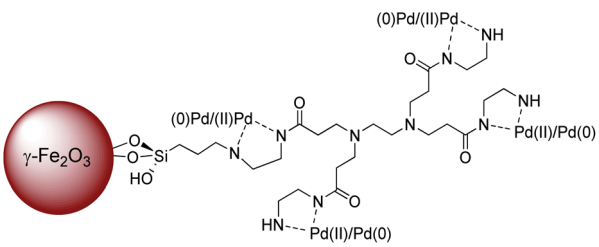

Fig. 1 The proposed structure of PAMAM G_0-Pd@γ-Fe_2O_3.

2.1 General procedure for the Suzuki–Miyaura cross-coupling reaction (9a–r)

PAMAM G_0-Pd@γ-Fe_2O_3 (0.47 mol%, 0.007 g) was added to a mixture of K_2CO_3 (2 mmol), phenylboronic acid (1.2 mmol), and aryl halide (1.0 mmol) in water (2 mL), under stirring and heated at 60 °C (90 °C when we used aryl chlorides). The progress of reaction was monitored by TLC until completion (15 min), then the nanocatalyst was separated by an external magnet. The reaction mixture was extracted with ethyl acetate (3 × 5 mL), and the combined organic layers were dried over anhydrous Na_2SO_4 and concentrated. The residue was purified on silica to give rise to the pure products **9a–r**.

2.2 General procedure for the Mizoroki–Heck cross-coupling reaction (12a–r)

PAMAM G_0-Pd@γ-Fe_2O_3 (0.61 mol%, 0.009 g) was added to a mixture of K_2CO_3 (2 mmol), alkene (1.5 mmol), and aryl halide (1.0 mmol) in water (2 mL), under stirring and heated at 80 °C (90 °C when we used aryl chlorides). The reaction progress was screened by TLC at different time intervals. After the completion of the reaction, the nanocatalyst was separated by an external magnet. The reaction mixture was extracted with ethyl acetate (3 × 5 mL), and the combined organic layers were dried over anhydrous Na_2SO_4 and concentrated. The residue was purified on silica to give rise to the pure products **12a–r**.

3. Results and discussion

3.1 Synthesis and characterization of the PAMAM G_0-Pd@γ-Fe_2O_3 MNPs

The successful synthesis of PAMAM G_0-Pd@γ-Fe_2O_3 was established by comparing its XRD pattern with those of γ-Fe_2O_3. The XRD pattern of γ-Fe_2O_3 (Fig. 2) confirms the cubic magnetite crystal structure according to the peaks at 15, 23.1, 26.9, 30.3, 35.8, 43.6, 50, 54.8, 57.3, 63.2, 71.1, and 74.4° (2θ), corresponding to the (110), (210), (211), (220), (311), (400), (421), (422), (511), (440), (620) and (533) miller indices respectively

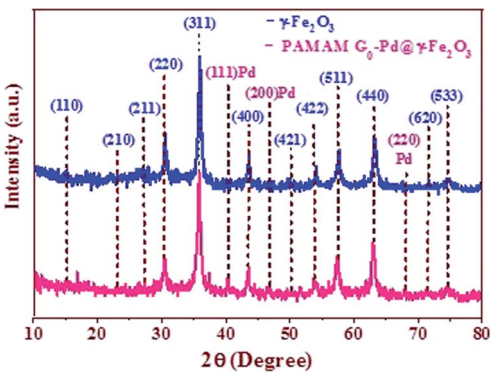

Fig. 2 XRD patterns of γ-Fe_2O_3, and PAMAM G_0-Pd@γ-Fe_2O_3 complex.

(JCPDS card no. 39-1346).[43,44] The unit cell is assigned as the space group $P4_132$ with the crystallographic parameters $a = b = c = 8.3515$ Å, and $\alpha = \beta = \gamma = 90°$. The observed diffraction peaks of PAMAM G_0-Pd@γ-Fe_2O_3 at 40.1, 46.7 and 68.1° (2θ) are attributed to the standard crystallographic pattern of Pd NPs corresponding to the (111), (200), and (220) miller indices (JCPDS Card no. 65-2867, Fig. 2).[45,46] The decrease of the XRD peak intensity of PAMAM G_0-Pd@γ-Fe_2O_3 can be attributed to the formation of palladium complexes on the surface of γ-Fe_2O_3 MNPs being stabilized by various functional groups present in the PAMAM dendrimer acting as ligands.

The FE–SEM images of γ-Fe_2O_3 NPs, γ-Fe_2O_3-CPTES and supported catalyst were shown in Fig. S10.† According to the FE-SEM images, the γ-Fe_2O_3 and γ-Fe_2O_3-CPTES NPs have a uniform spherical morphology (Fig. S10A†). Also, the particles of the supported catalyst on the surface of γ-Fe_2O_3 NPs have a homogeneous spherical morphology and uniform size distribution. This clearly shows the synergistic effect of organic and inorganic diverse ingredients in a homogeneous network of PAMAM G_0-Pd@γ-Fe_2O_3 (**6**) (Fig. S10B†).

The TEM image of PAMAM G_0-Pd@γ-Fe_2O_3 is in line with the proposed core–shell structure placing palladium nanoparticles at the surface of magnetic Fe_2O_3 nanoparticles (Fig. 3). Energy-dispersive X-ray (EDX) choosing a point at random on the surface of PAMAM G_0-Pd@γ-Fe_2O_3 NPs (Fig. 4) confirmed the presence of Pd, N, O, Si, Fe, Cl, and C, in 8.10, 7.74, 21.03, 2.45, 43.79, 2.69, and 14.20 wt% respectively.

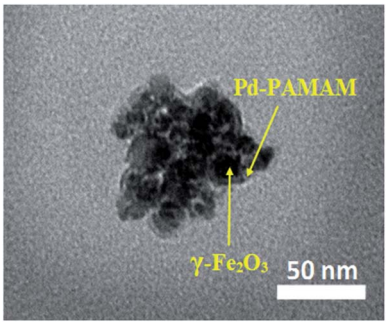

Fig. 3 TEM images of the PAMAM G_0-Pd@γ-Fe_2O_3 complex.

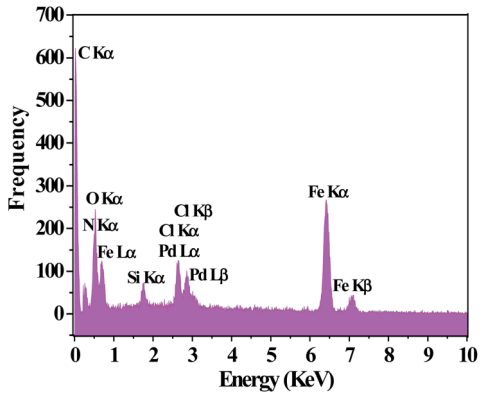

Fig. 4 EDX analysis of the PAMAM G_0-Pd@γ-Fe_2O_3 complex.

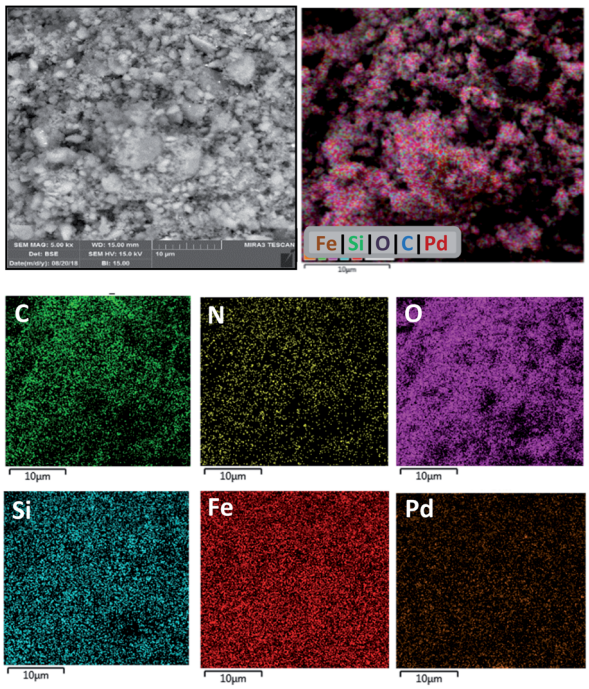

Fig. 5 EDS elemental mappings of the PAMAM G_0-Pd@γ-Fe_2O_3 complex.

Elemental mapping analysis by energy dispersive spectroscopy (EDS) of PAMAM G_0-Pd@γ-Fe_2O_3 (Fig. 5) indicates that Pd NPs are distributed almost uniformly and without aggregation

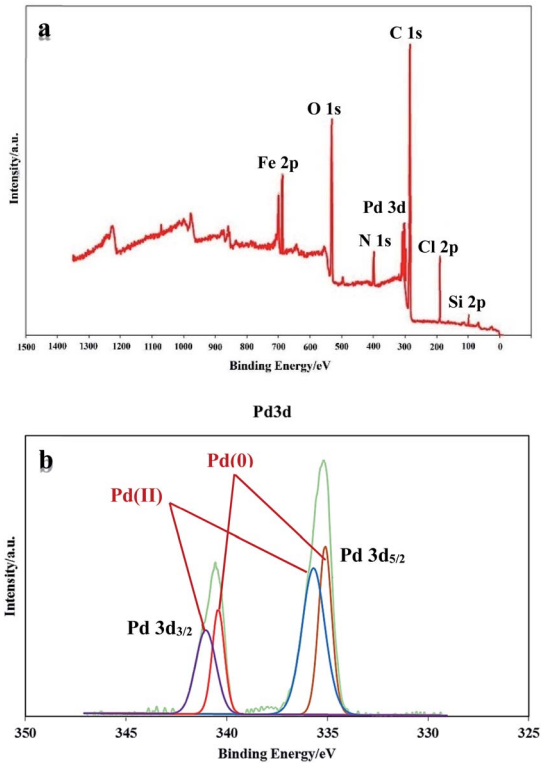

Fig. 6 XPS patterns of PAMAM G_0-Pd@γ-Fe_2O_3: overall elemental survey spectrum (a), and, Pd3d (b).

Table 1 Suzuki–Miyaura cross-coupling reactions of different aryl halides with phenylboronic acid catalyzed by PAMAM G_0-Pd@γ-Fe_2O_3[a]

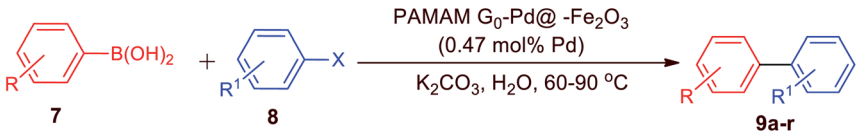

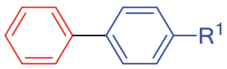

Prod.	X	R^1	Yield	t (min)	TON	TOF
9a	I	NH_2	85	120	180	90
9a	Cl	NH_2	65	150	138	39
9b	I	OMe	92	70	195	168
9b	Br	OMe	90	110	191	104
9c	I	Me	85	90	180	120
9c	Br	Me	75	120	159	79
9c	Cl	Me	65	150	138	55
9d	I	H	95	15	202	808
9d	Br	H	95	20	202	612
9d	Cl	H	92	100	195	117
9e	I	CHO	93	60	197	197
9e	Br	CHO	85	85	180	128
9e	Cl	CHO	75	100	195	96
9f	Br	COMe	95	90	202	134
9g	I	NO_2	94	25	200	487
9g	Br	NO_2	90	35	191	330
9g	Cl	NO_2	87	55	155	155
9h	Br	CN	80	90	170	113
9h	Cl	CN	60	180	148	49

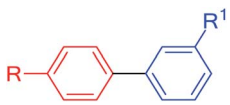

Prod.	X	R	R^1	Yield	t (min)	TON	TOF
9i	I	H	NH_2	75	120	180	90
9j	Br	H	CF_3	90	40	191	290
9k	Br	OMe	NO_2	90	50	191	230
9l	Br	Me	NO_2	92	60	195	195
9m	I	H	NO_2	94	50	200	240
9n	Br	NO_2	NO_2	90	50	191	230

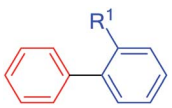

Prod.	X	R^1	Yield	t (min)	TON	TOF
9o	Br	Me	75	120	159	80
9o	Cl	Me	60	220	127	34
9p	I	COOH	94	30	200	400
9p	Br	COOH	90	60	191	191
9p	Cl	COOH	80	80	170	85
9q	I	NO_2	80	60	170	170

Table 1 (*Contd.*)

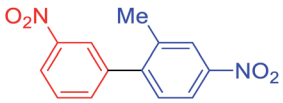

Prod.	X	Yield	*t* (min)	TON	TOF
9r	I	85	80	180	135

[a] Reaction conditions: phenylboronic acid (1.2 mmol), aryl halide (1.00 mmol), K_2CO_3 (Et_3N when we used the aryl chlorides) (2.00 mmol), catalyst (0.007 g, 0.47 mol% of Pd), H_2O (2.0 mL), 60 °C (90 °C when we used the aryl chlorides); all yields are isolated.

Table 2 Mizoroki–Heck cross-coupling reactions of different aryl halides with styrene catalyzed by PAMAM G_0-Pd@γ-Fe_2O_3[a]

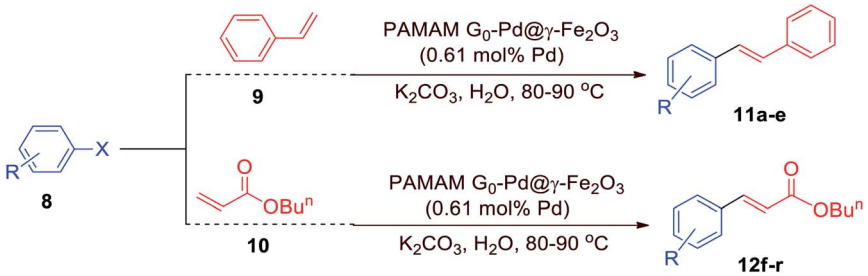

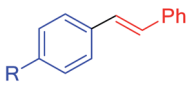

Prod.	X	R	Yield	*t* (min)	TON	TOF
12a	I	Me	75	180	122	41
12a	Br	Me	65	180	106	35
12a	Cl	Me	55	220	90	24
12b	I	OMe	90	90	148	98
12c	I	H	95	60	155	150
12c	Br	H	95	80	155	117
12c	Cl	H	90	120	147	73
12d	I	CN	85	60	139	139
12e	I	NO_2	95	45	155	206
12e	Br	NO_2	95	50	155	186
12e	Cl	NO_2	90	60	147	147

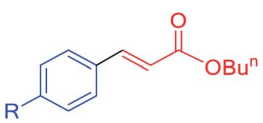

12f	I	OH	90	120	147	73
12g	I	NH_2	90	120	147	73
12h	I	OMe	92	500	150	181
12h	Cl	OMe	65	300	106	21
12i	I	Me	80	120	131	65
12i	Br	Me	80	140	131	56
12i	Cl	Me	70	150	114	45
12j	I	H	95	50	155	187
12j	Br	H	90	75	147	117
12j	Cl	H	80	100	131	78
12k	I	Cl	85	55	139	153
12k	Br	Cl	70	60	114	114

Table 2 (*Contd.*)

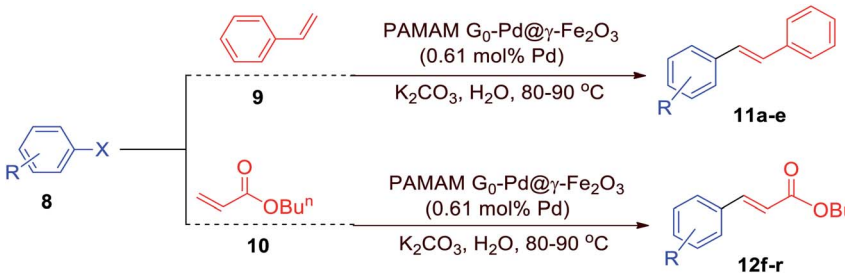

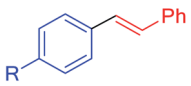

Prod.	X	R	Yield	*t* (min)	TON	TOF
12l	I	Br	75	70	122	105
12m	I	CO_2Et	95	40	131	65
12m	Br	CO_2Et	93	50	152	183
12m	Cl	CO_2Et	90	80	147	110
12n	I	COMe	92	70	150	129
12o	Br	CN	92	50	150	181
12o	Cl	CN	85	120	139	69
12p	I	NO_2	95	30	155	77

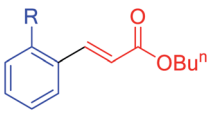

12q	Br	Me	65	130	106	49
12q	Cl	Me	50	240	81	20
12r	I	NO_2	92	70	150	129

[a] Reaction conditions: styrene or *n*-butyl acrylate (1.5 mmol), aryl halide (1.00 mmol), K_2CO_3 (Et_3N when we used the aryl chlorides) (2.00 mmol), catalyst (0.009 g, 0.61 mol% of Pd), H_2O (2.00 mL), 80 °C (90 °C when we used aryl chlorides); all yields are isolated.

on the catalyst surface along with the other elements (C, N, O, Si, Fe) present.

XPS analysis was performed to investigate the chemical state of the surface of PAMAM G_0-Pd@γ-Fe_2O_3 (Fig. 6a). In the XPS elemental survey of PAMAM G_0-Pd@γ-Fe_2O_3, the peaks corresponding to carbon, oxygen, nitrogen, chlorine, silicon, palladium and iron are clearly observed (Fig. 6a). Also, Pd(0)/(II) existence in the catalyst structure were confirmed through XPS analysis through studying binding energy range of 335.15 to 340.97 eV (Fig. 6b). As shown in Fig. 6b, the peaks located at 335.15 (3d5/2) and 340.35 eV (3d3/2) correspond to Pd(II) species, and also the peaks appeared at 336.11 (3d5/2) and 340.97 eV (3d3/2) are attributed Pd(II) (Fig. 6b). According to XPS results, the ratio of Pd(0)/Pd(II) is equal to 0.40 (in atomic number).

3.2 Evaluation of the catalytic activity of PAMAM G_0-Pd@γ-Fe_2O_3 MNPs in cross-coupling reactions

Taking the Suzuki–Miyaura C–C coupling reaction between iodobenzene and phenylboronic acid as the model reaction, PAMAM G_0-Pd@γ-Fe_2O_3 was evaluated varying solvent, temperature, base, and catalyst loading (see ESI for details, Fig. S17†), suggesting that the best results were achieved with polar solvents. Being green and safe, we were pleased to see that the reaction proceeded exceptionally well in water, giving rise to 95% yield with a catalyst loading of 0.47 mol% within 15 minutes of reaction time at 60 °C.

With the optimized reaction conditions in hand, we evaluated the substrate scope of PAMAM G_0-Pd@γ-Fe_2O_3 for Suzuki–Miyaura coupling reactions (Table 1). A wide variety of electron-deficient or electron-rich aryl halides or phenylboronic acids were amenable, and functional groups that could be potentially sensitive under the basic, aqueous reaction conditions employed (CHO, CN, NH_2) were tolerated well. As expected, the reactivity decreased from aryl iodides *via* aryl bromides to aryl chlorides, but even for the latter high yields could be obtained by raising the reaction temperature to 90 °C and prolonging the reaction time 100–220 min.

Analogously, the catalytic activity of PAMAM G_0-Pd@γ-Fe_2O_3 was evaluated for Mizoroki–Heck C–C coupling reactions.

Screening of conditions for the reaction of iodobenzene with styrene (see ESI for details, Fig. S18†) also revealed for this transformation water to be a suitable choice in combination with K_2CO_3 at a reaction temperature of 80 °C, giving rise to 1,2-diphenylethylene in 95% yield within 60 minutes at a catalyst loading of 0.61 mol%.

Evaluating the substrate scope under the optimized reaction conditions demonstrated that a great variety of electronically and sterically differentiated aryl halides reacted smoothly in the coupling with styrene or *n*-butyl acrylate (Table 2). Noteworthy, electron-rich and electron-poor aryl chlorides could be converted, requiring only slightly longer reaction times and higher temperatures (90 °C).

Control experiments confirmed for both, the Suzuki–Miyaura as well as the Mizoroki–Heck reactions that no coupling is observed with the parent materials PAMAM G_0@γ-Fe_2O_3 and PAMAMG_0, but also that $PdCl_2$ as a stand-alone catalyst does not promote the transformations. The high activity and efficiency of the PAMAM G_0-Pd@γ-Fe_2O_3 catalyst compares well to other catalysts examined for comparison (see Fig. S19†).

3.3 Recyclability study

The recyclability, activity, and stability of PAMAM G_0-Pd@γ-Fe_2O_3 catalyst were examined using the hot-filtration method taking the Mizoroki–Heck reaction between iodobenzene and styrene (Table 2, entry 5) as a representative example.

After the catalyst was magnetically removed from the reaction medium (28 min, 50% yield of 1,1-diphenylethylene monitored by GC), the reaction, by and large, did not proceed further (53% yield after 90 min, Fig. S20†), indicating that little to no catalytically active species were present outside the support.

ICP analysis of the Mizoroki–Heck model reaction solution was performed to determine the amount of palladium leaching for six consecutive catalytic runs (Fig. S21†).

Base on the results, Pd catalyst, showed high stability, with little leaching of Pd (total less than 1%), while consistent yields (95–93%) of 1,1–diphenylethylene were obtained for each cycle (see ESI for details, Table S1†).

Likewise, recyclability of the PAMAM G_0-Pd@γ-Fe_2O_3 complex was evaluated for the Suzuki–Miyaura reaction between iodobenzene and phenylboronic acid for 6 sequential runs (see ESI for details, Table S1†), giving rise to 93–95% yield in each run. The comparison of TEM and SEM images of fresh and the used catalyst after 6 runs in the Mizoroki–Heck reaction did not show significant changes in size and morphology (Fig. 7a and b). In addition, VSM measurements (Fig. 7c) and FT-IR spectra (Fig. 7e) further confirmed that the catalyst did not change in its structure and magnetic properties. Also, evaluation and comparison leaching, some of hydrophilic/

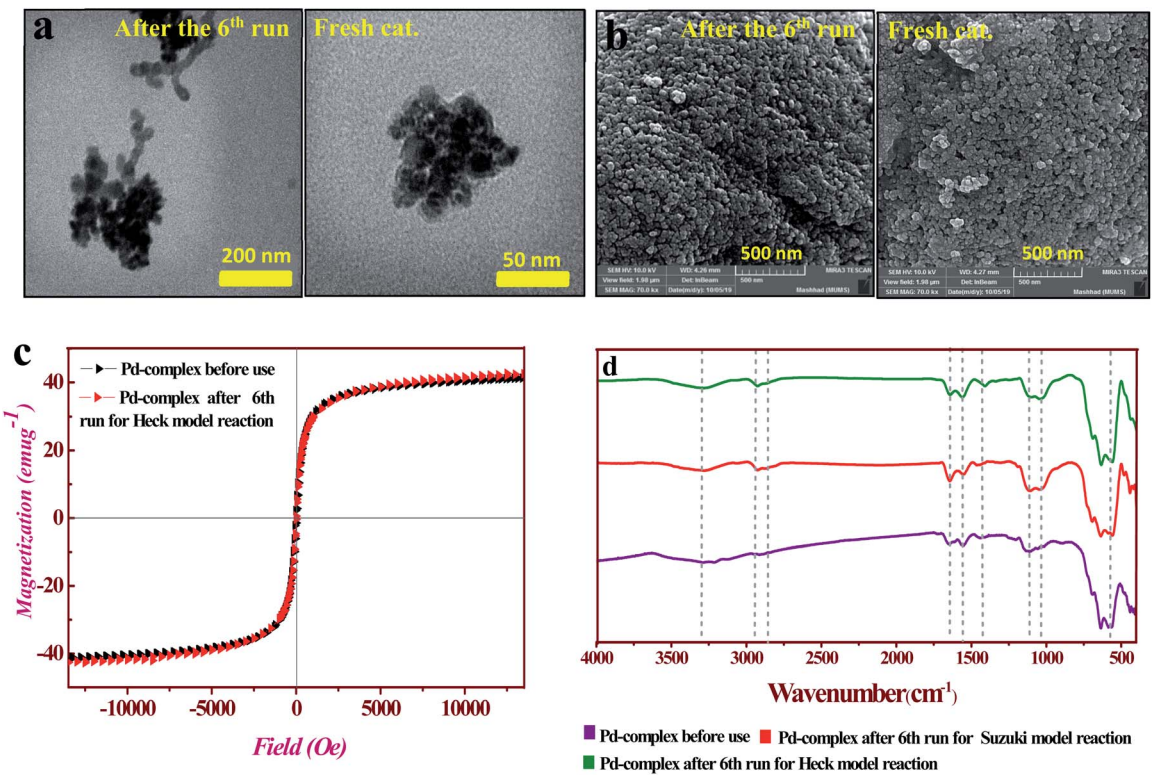

Fig. 7 7(a) TEM, and (b) FE-SEM, images recovered of the PAMAM G_0-Pd@γ–Fe_2O_3 complex after the 6th run for the model reaction of Mizoroki–Heck; (c) magnetization curves of PAMAM G_0-Pd@γ-Fe_2O_3 before use and PAMAM G_0-Pd@γ-Fe_2O_3 after the 6th run for the model reaction of Mizoroki–Heck, at 300 K; (d) FT-IR spectra of PAMAM G_0-Pd@γ-Fe_2O_3 before use; FT-IR spectra of PAMAM G_0-Pd@γ-Fe_2O_3 after 6th run for the model reactions of Suzuki–Miyaura and Mizoroki–Heck cross-couplings.

amphiphilic catalysts effective in c–c cross coupling reactions with PAMAM G_0-Pd@γ-Fe_2O_3 catalyst were performed to better understand the activity of the PAMAM G_0-Pd@γ-Fe_2O_3 (see Table 3. ESI† for found more details).

4. Summary and conclusions

In conclusion, we developed a recyclable magnetic nano Pd-complex, formulated as PAMAM G_0-Pd@γ-Fe_2O_3 MNPs, which proved to be an efficient catalyst for the Suzuki–Miyaura and Mizoroki–Heck coupling. Notable features are its high activity in water, which allows the employment of aryl chloride at moderately forcing conditions (90 °C), facile recyclability and reuse, as well as little palladium leaching (<1% in a total of 6 runs).

Conflicts of interest

All the authors, declare that they haven't any of conflicts of interest.

Acknowledgements

Authors gratefully acknowledge the financial support by the Research Council of University of Birjand, Birjand, Iran and Hakim Sabzevari University, Sabzevar, Iran.

References

1 R. Karu and S. Gedu, *Green Chem.*, 2018, **20**, 369–374.
2 P. Slavík, D. W. Kurka and D. K. Smith, *Chem. Sci.*, 2018, **9**, 8673.
3 O. Al-Madanat, Y. AlSalka, M. Curti, R. Dillert and D. W. Bahnemann, *ACS Catal.*, 2020, **10**, 7398–7412.
4 W. Ji, H.-H. Wu and J. Zhang, *ACS Catal.*, 2020, **10**, 1548.
5 L. Zhou, S. Li, B. Xu, D. Ji, L. Wu, Y. Liu, Z. M. Zhang and J. Zhang, *Angew. Chem., Int. Ed.*, 2020, **59**, 2769.
6 H. Lee, Y. Lee and S. H. Cho, *Org. Lett.*, 2019, **21**, 5912.
7 I. V. Gürsel, T. Noël, Q. Wang and V. Hessel, *Green Chem.*, 2015, **17**, 2012.
8 L. Stadler, M. Homafar, A. Hartl, S. Najafishirtari, M. Colombo, R. Zboril, P. Martin, M. B. Gawande, J. Zhi and O. Reiser, *ACS Sustainable Chem. Eng.*, 2018, **7**, 2388.
9 S. Wittmann, J.-P. Majoral, R. N. Grass, W. J. Stark and O. Reiser, *Green Process. Synth.*, 2012, **1**, 275.
10 D. J. Snelders, G. van Koten and R. J. Klein Gebbink, *J. Am. Chem. Soc.*, 2009, **131**, 11407.
11 Y. Yu, T. Hu, X. Chen, K. Xu, J. Zhang and J. Huang, *Chem. Commun.*, 2011, **47**, 3592.
12 F. Wang, J. Mielby, F. H. Richter, G. Wang, G. Prieto, T. Kasama, C. Weidenthaler, H. J. Bongard, S. Kegnæs and A. Fürstner, *Angew. Chem., Int. Ed.*, 2014, **126**, 8789.
13 J. Zhi, D. Song, Z. Li, X. Lei and A. Hu, *Chem. Commun.*, 2011, **47**, 10707.
14 L. Wu, B.-L. Li, Y.-Y. Huang, H.-F. Zhou, Y.-M. He and Q.-H. Fan, *Org. Lett.*, 2006, **8**, 3605.
15 A. L. Isfahani, I. Mohammadpoor-Baltork, V. Mirkhani, A. R. Khosropour, M. Moghadam, S. Tangestaninejad and R. Kia, *Adv. Synth. Catal.*, 2013, **355**, 957.
16 E. Mulahmetovic and G. Hargaden, *Rev. J. Chem.*, 2017, **7**, 373.
17 Z. B. Shifrina, V. G. Matveeva and L. M. Bronstein, *Chem. Rev.*, 2019, **120**, 1350.
18 J. Blümel, *Coord. Chem. Rev.*, 2008, **252**, 2410.
19 N. E. Leadbeater and M. Marco, *Chem. Rev.*, 2002, **102**, 3217.
20 S. Sobhani and Z. Pakdin-Parizi, *Appl. Catal., A*, 2014, **479**, 112.
21 R. N. Baig and R. S. Varma, *Green Chem.*, 2013, **15**, 398.
22 R. N. Baig, J. Leazer and R. S. Varma, *Clean Technol. Environ. Policy*, 2015, **17**, 2073.
23 M. Nasrollahzadeh, Z. Issaabadi and R. S. Varma, *ACS Omega*, 2019, **4**, 14234.
24 R. Luque, B. Baruwati and R. S. Varma, *Green Chem.*, 2010, **12**, 1540.
25 A. K. Rathi, M. B. Gawande, J. Pechousek, J. Tucek, C. Aparicio, M. Petr, O. Tomanec, R. Krikavova, Z. Travnicek and R. S. Varma, *Green Chem.*, 2016, **18**, 2363.
26 M. Nasrollahzadeh, S. M. Sajadi, A. Rostami-Vartooni and M. Khalaj, *J. Mol. Catal. A: Chem.*, 2015, **396**, 31.
27 M. B. Gawande, P. S. Branco and R. S. Varma, *Chem. Soc. Rev.*, 2013, **42**, 3371.
28 R. Sedghi, B. Heidari, H. Shahmohamadi, P. Zarshenas and R. S. Varma, *Molecules*, 2019, **24**, 3048.
29 V. Polshettiwar, R. Luque, A. Fihri, H. Zhu, M. Bouhrara and J.-M. Basset, *Chem. Rev.*, 2011, **111**, 3036.
30 R. Ye, A. V. Zhukhovitskiy, C. V. Deraedt, F. D. Toste and G. A. Somorjai, *Acc. Chem. Res.*, 2017, **50**, 1894.
31 C. Gao, F. Lyu and Y. Yin, *Chem. Rev.*, 2021, **121**(2), 834–881.
32 Y. Zhou, L. Luan, B. Tang, Y. Niu, R. Qu, Y. Liu and W. Xu, *Chem. Eng. J.*, 2020, **398**, 125651.
33 M. R. Nabid, Y. Bide and S. J. T. Rezaei, *Appl. Catal., A*, 2011, **406**, 124.
34 X. Yan, Y. Luo, W. Liu, L. Liang, Y. Gan, Z. Chen, Z. Xu, H. Wan, D. Tang and H. Shi, *Phys. Chem. Chem. Phys.*, 2020, **22**, 6222.
35 Y. Zhang, X. Wei and Z. Yao, *Chin. J. Chem.*, 2010, **28**, 2274.
36 R. Ma, P. Yang and F. Bian, *New J. Chem.*, 2018, **42**, 4748.
37 J. Lemo, K. Heuzé and D. Astruc, *Org. Lett.*, 2005, **7**, 2253.
38 Y. Yang, S. Ogasawara, G. Li and S. Kato, *Polym. J.*, 2015, **47**, 340.
39 E. Niknam, A. Moaddeli and A. Khalafi-Nezhad, *J. Organomet. Chem.*, 2020, **923**, 121369.
40 N. Bahri-Laleh, S. Sadjadi and A. Poater, *J. Colloid Interface Sci.*, 2018, **531**, 421.
41 F. Giacalone, V. Campisciano, C. Calabrese, V. La Parola, Z. Syrgiannis, M. Prato and M. Gruttadauria, *ACS Nano*, 2016, **10**, 4627.
42 J. Lemo, K. Heuzé and D. Astruc, *Inorg. Chim. Acta*, 2006, **359**, 4909.
43 E. Darezereshki, *Mater. Lett.*, 2010, **64**, 1471.
44 V. Sreeja and P. Joy, *Mater. Res. Bull.*, 2007, **42**, 1570.
45 K. Cheng, D. Cao, F. Yang, L. Zhang, Y. Xu and G. Wang, *J. Mater. Chem.*, 2012, **22**, 850.
46 J. Cui, N. Zhu, N. Kang, C. Ha, C. Shi and P. Wu, *Chem. Eng. J.*, 2017, **328**, 1051.